International Journal of Sciences: Basic and Applied Research (IJSBAR)

ISSN 2307-4531
(Print & Online)

https://gssrr.org/index.php/JournalOfBasicAndApplied/index

Synchronization of Chaotic Oscillators Operating in the UHF Band Using the Adaptive Observer Method

Franklin Djimasra[a*], Jean De Dieu Nkapkop[b], Nestor Tsafack[c], Abdelkrim Boukabou[d], Jean Yves Effa[e]

[a]*Department of Fundamental Sciences, University of Moundou, B.P. 206 Moundou, Tchad*

[b]*Department of Electrical Engineering and Industrial Computing, University Institute of Technology, P.O. Box 8698 Douala, Cameroon*

[c]*Research Unit of Laboratory of Condensed Matter, Electronics and Signal Processing(URMACETS)*

[d]*Department of Physics, Faculty of Sciences, University of Dschang, P.O. Box 67, Dschang, Cameroon*

[e]*Department of Electronics, University of MSB Jijel, Ouled Aissa, Jijel 18000, Algeria*

[a]*Email: masrafranck@gmail.com,*[b]*Email: jdd.nkapkop@gmail.com*

[c]*Email: nestor.tsafack@yahoo.fr,*[d]*Email: aboukabou@gmail.com*

[e]*Email: effa_jo@gmail.com*

Abstract

In this work, we consider the synchronization between chaotic oscillators with different orders and operating in the UHF band. Firstly, the normalized state equation of Hartley and Colpitts oscillators are presented as well as their chaotic behavior has been proven in this frequency band. Secondly, the problem of dynamics synchronization is investigated, and a controller based on Lyapunov stability theory is proposed to ensure synchronization between both oscillators. Finally, computer experiments are provided to demonstrate the effectiveness and feasibility of the proposed synchronization approach.

Keywords*:* Chaos; synchronization; Hartley oscillator; Colpitts oscillator; UHF band.

Received: *11/16/2025*
Accepted: *1/16/2026*
Published: *1/26/2026*

---

* *Corresponding author.*

1. Introduction

Chaos synchronization refers to a process wherein two (or many) chaotic systems (either identical or non-identical) adjust a given property of their motion to a common behavior due to coupling or forcing. The idea of synchronizing chaotic systems with different initial conditions was introduced by Pecora and Carroll in 1990 [1]. Since then, there has been a particular interest in chaotic synchronization, due to many potential applications in secure communication [2]. Hence, in order to recover the information, the chaotic generator (drive system) in the transmitter must be synchronized with the generator (response system) in the receiver. Many other fields have been subject of chaos synchronization such as chemical and biological systems [3,4].

On the other hand, the study of chaotic oscillators to information technologies [10] is under intensive investigation. In this frame, there is a great interest behind the study of chaotic oscillator operating at high MHz frequencies, due to their potential applications in future communication systems [11], and in radar systems [12]. In particular, it has been shown that the Colpitts oscillator, with special settings of the circuit parameters can exhibit chaotic behavior. This circuit was investigated at the kHz frequencies [5], high (3-300MHz) frequencies [6] and ultrahigh (300-1000 MHz) frequencies [7] both numerically and experimentally. At the same time, it has been shown that Hartley oscillator, according to the general architecture of circuit parameters structures can produce chaotic behavior [8].

To synchronize chaotic oscillators, a huge variety of methods have been developed such as nonlinear Pecora-Carroll method [13,14], linear coupling technique [11,15,16], adaptive synchronization [17], active control synchronization [18], linear feedback control method [19], observer-based synchronization [20] and so on. Note that most of the aforementioned methods investigated the chaos synchronization for identical chaotic oscillators however, both Colpitts and Hartley chaotic oscillators may be identical [11,12,14-16,18-20] or non-identical with different parameters in most cases [16,17]. Recently, a lot of effort has been devoted to synchronize a class of chaotic systems in the presence of system's disturbances and unknown parameters [21, Boukabou,. . .]. Especially, the adaptive observer based synchronization concept has attracted increased interests among the others since it presents the advantage that the full state vector estimation of system's disturbances and unknown parameters, and chaos synchronization can be achieved simultaneously. Thus, it is important and interesting to investigate chaos synchronization behavior between non-identical Hartley and Colpitts oscillators using the adaptive observer method. Although, the method of the synchronization of two different chaotic oscillators is far from being straightforward, in this work, we address the problem of chaos synchronization between two non-identical chaotic oscillators with different orders designed to operate in the UHF band. This is numerically investigated by means of integration of simplified (piecewise-linear) different equations. Following the concept of adaptive observer based synchronization [22], we address the problem of dynamics synchronization using a controller based on Lyapunov stability theory to ensure synchronization between non-identical Hartley and Colpitts oscillators. Finally, computer experiments are provided to demonstrate the effectiveness and feasibility of the proposed synchronization approach. It is worth noting that the use of the electronic Hartley and Colpitts oscillators is due to the following reasons: On the first hand, the Hartley oscillator uses a tapped coil and a diode as maintenance circuit in the sense that the presence of an internal current source in the JFET explains its active behavior and produces the chaotic behavior in autonomous operation. The non-linearity in this circuit comes from the effect of

the diode. On the other hand, the Colpitts oscillator uses a simple transistor as maintenance circuit; it has an

intrinsic non-linearity due to the bipolar transistor (BJT) and it was a diversified dynamic behavior. The frequency range of this later oscillator can vary from a few hertz to UHF band, and hence, solicited in electronic devises and communication systems.The remainder of this paper is organized as follows. In Section 1, the circuit models for Hartley and Colpitts oscillators are introduced, and the normalized state equations are presented while their chaotic behavior is confirmed. In Section 2, the synchronization state of chaotic oscillators with different orders is addressed using the adaptive observer method. Lyapunov stability theory to ensure synchronization between non-identical Hartley and Colpitts oscillators are proven. In Section 4, computer experiments are investigated to validate this approach. Finally, Section 5 concludes the paper.

2. Circuit and basic equations of oscillators

In this section, we briefly introduce the circuits under investigations and give their corresponding state space equations.

2.1. Chaotic dynamic of Hartley oscillator

Figure 1 represents the oscillator consisting of a $JFET$ and a tapped coil [23]. The control parameter of this oscillator is the bias voltage source connected to the circuit between the drain (D) of the $JFET$ and the ground. In case if the control parameter has to be different from the bias voltage source, variable inductors may be used at the place of the tapped coil. Otherwise, the circuit has to be upgraded to a three-component chaos generating Hartley's oscillator by the insertion of a variable resistor. In this later case, chaos will occur only for low values of that resistance, in the range of some few ohms, if this is mounted in series with the source (S) or with the gate (G) of the $JFET$. The value of the connected resistance is considered as the control parameter. It should be noted that, this later equal to zero, then the circuit will behave like the two-component circuit in discussion in this paper. The resistance can also be connected in parallel to one side of the tapped coil, for instance between (G) and (S) of the $JFET$ or between (S) and the ground. In that case, for the circuit to generate chaotic behavior, the value of the resistance has to be in the range of hundreds of kilo Ohms. For very high values of the resistance, the circuit will again function as a two-component circuit, since the current passing through the resistor will be negligible as if the circuit were opened at that point.

To model the circuit, we have considered some simplifications: (i) The internal resistance of the tapped coil is neglected; (ii) Because of the low voltage and low power in the circuit, currents in the different branches of the tapped coil are also low, and therefore, the magnetic field generated by each side of this tapped coil is too weak to generate a no negligible magnetic coupling between the two branches; (iii) As a result of the previous point, we are going to use the high-frequency small-signal equivalent circuit model of a $JFET$ as proposed by Elshabini [9]. In this model, the capacitance of the parasitic capacitor between the drain and the source is neglected

to the advantage of the two others which are greater. The voltage at the drain is globally higher than that at the gate of the $JFET$, making the diode at the junction gate-drain with its anode at the gate to be permanently biased in the reverse sense. So, it is not part of modeling. Thus, the system still respects the low-order oscillators according to the architecture of general structures for autonomous chaotic oscillators proposed by Elwakil and Kennedy [8]. The presence of internal current sources in the $JFET$ explains its active behavior and thus, the simple architecture of the model presented here can exhibit chaos while functioning autonomously [26].

The state equations governing the above electrical circuit (Fig. 1) are derived from Kirchhoff laws as:

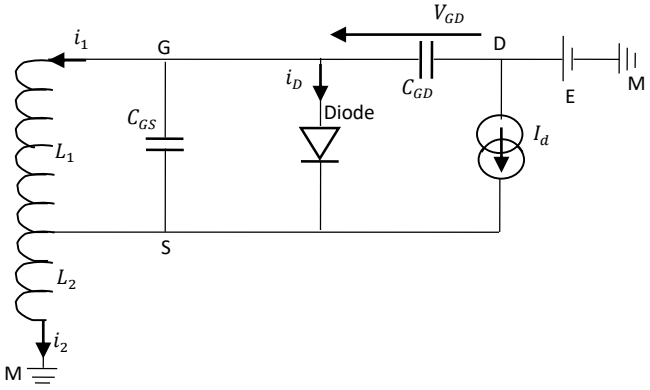

Figure 1: Equivalent circuit of Hartely oscillator using the simplified Giacoletto dynamic model of the $JFET$ for small signals at high frequency according to reference [9].The parasitic capacitor between the drain and the source is neglected as well as the diode effect between the gate and the drain of the $JFET$

$$\begin{cases} C_{GS}\dfrac{dv_{GS}}{dt} = i_2 - I_d - i_1 - i_D \\ C_{GD}\dfrac{dv_{GD}}{dt} = I_d - i_2 \\ L_1\dfrac{di_1}{dt} = v_{GS} \\ L_2\dfrac{di_2}{dt} = -v_{GS} + v_{GD} + E \end{cases} \quad (1)$$

Where, *E* is the bias voltage source and the control parameter of the system at the same time. L_1 and L_2 are the inductances of the two inductors formed by the tapped coil. In the set of $Eq.(1)$ the i_h with $h \in \{1,2\}$ represent the currents flowing through the inductor parts L_1 and L_2, while v_{GS} and v_{GD} respectively correspond to the voltages across the parasitic capacitors C_{GS} and C_{GD}. The voltage v_{GS} across the gate-source junction of the $JFET$ is equal to the potential difference between the anode and the cathode of the diode.

Consequently, the expression of the current flowing through that diode is expressed by

$$i_D = I_S\left[\exp\left(\frac{v_{GS}}{V_T}\right)-1\right] \tag{2}$$

where I_S its reverse saturation's current.

The nonlinearities in this electrical model arise in the circuit from the diodes effect at the $p-n$ junction gate-source, which is characterized by its current i_D, as well as from the current source between the drain and the source. The simplified mathematical modeling of the later, that is to say the nonlinear current I_d flowing from the drain to the source can be described by the following set of equations showing the functioning of the $JFET$ in the cutoff, the saturation and the triode regions [24]

$$I_d = \begin{cases} 0 & if \quad v_{GS} \le V_{GSoff} \\ g_{m0}\left(v_{GS}-v_{GSoff}\right)^2 & if \quad v_{GD} \le V_{GSoff} \\ g_{m0}\left(v_{GS}-v_{GD}\right)\left(v_{GS}+v_{GD}-2v_{GSoff}\right) & if \quad v_{GD} \ge V_{GSoff} \end{cases} \tag{3}$$

where $V_{GSoff} \le 0$ is the cutoff value of the voltage between the gate and the source; g_{m0} is the current gain of the $JFET$. Note that the voltages, currents and time can be normalized with respect to V_T, I_0 and $\tau = w_0 t$ respectively, where w_0 is the resonant radian frequency of the system.

Introducing the dimensionless states variables x_1, x_2, x_3 and x_4 such that $v_{GS} = V_T * x_1$, $v_{GD} = V_T * x_2$, $i_1 = I_0 * x_3$, $i_2 = I_0 * x_4$, the state $Eq.(1)$ discribing the system is then rewritten as follows:

where

$$a_1 = \frac{I_0}{V_T C_{GS} w_0},\ a_2 = \frac{I_S}{V_T C_{GS} w_0},\ a_3 = \frac{g_{m0V_T}}{C_{GS} w_0},\ b_1 = \frac{V_T}{L_1 I_0 w_0},\ b_2 = \frac{V_T}{L_2 I_0 w_0},\ \alpha = \frac{C_{GS}}{C_{GD}},\ e = \frac{E}{V_T}$$

$$a_1 = \frac{I_0}{V_T C_{GS} w_0},\ a_2 = \frac{I_S}{V_T C_{GS} w_0},\ a_3 = \frac{g_{m0} V_T}{C_{GS} w_0},\ b_1 = \frac{V_T}{L_1 I_0 w_0}, b_2 = \frac{V_T}{L_2 I_0 w_0},\ \alpha = \frac{C_{GS}}{C_{GD}},\ e = \frac{E}{V_T}$$

for $x_2 = y_1$, $x_3 = z_1$ et $x_4 = v_1$, then the equations (1) et (3) take the following form :

$$\begin{cases} \dot{x}_1 = a_1(v_1 - z_1) - a_2\left[\exp(x_1)-1\right] - a_3 g(x_1, y_1) \\ \dot{y}_1 = \alpha\left(a_1 v_1 - a_3 g(x_1, y_1)\right) \\ \dot{z}_1 = b_1 x_1 \\ \dot{v}_1 = b_2(e - x_1 + y_1) \end{cases} \tag{4}$$

The nonlinear function expressing the drain-source current takes now the normalized form in the following Equation (4) :

$$g(x_1, y_1) = \begin{cases} 0 & si \quad x_1 \le x_m \\ (x_1 - x_m)^2 & si \quad y_1 \le x_m \\ (x_1 - y_1)(x_1 + y_1 - 2x_m) & si \quad y_1 \ge x_m \end{cases} \qquad (6)$$

with $x_m = \dfrac{v_{GSoff}}{V_T} \le 0$

When the system parameters are chosen by… The simulated phase portrait in the plane (v_1, y_1, z_1) is given in Figure 2. Clearly, the system can exhibit chaotic behavior.

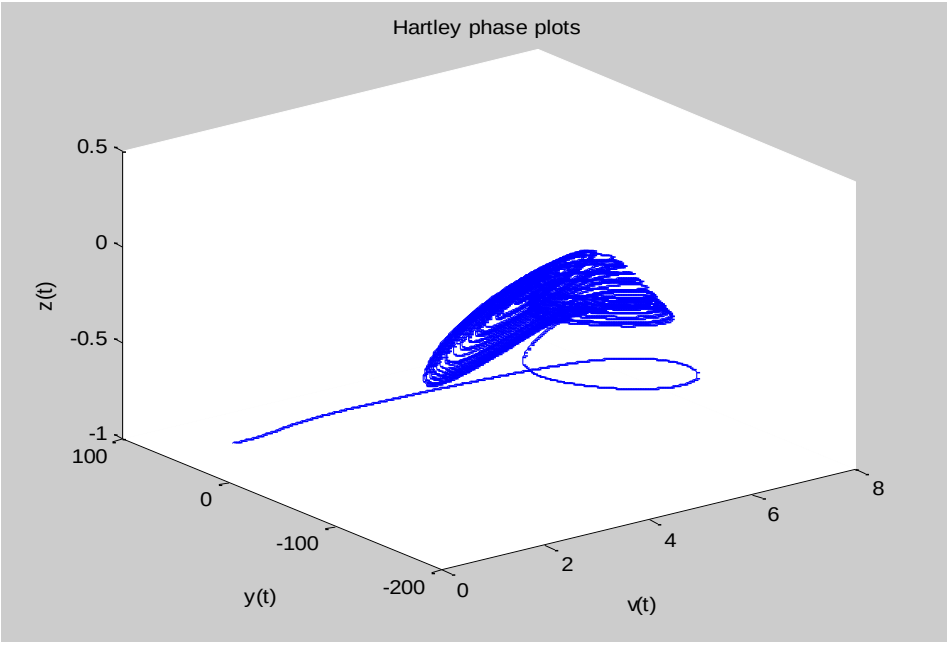

Figure 2: Phase portrait Hartley system

2.1.1. Equilibrium points and their nature

The equilibrium points are solutions of $Eq.(4)$ for $\dot{x}_k = 0, k \in \{1,...,4\}$. The system of equations to be solved becomes:

$$\begin{cases} 0 = a_1(v_1 - z_1) - a_2\left[\exp(x_1) - 1\right] - a_3 g(x_1, y_1) \\ 0 = \alpha\left(a_1 v_1 - a_3 g(x_1, y_1)\right) \\ 0 = b_1 x_1 \\ 0 = b_2(e - x_1 + y_1) \end{cases} \qquad (6)$$

The general form of the equilibrium points is recorded as $p_f = \left(x_1^* = 0, y_1^* = -e, z_1^* = 0, v_1^* = \frac{a_3}{a_1} g(x_1, y_1) \right)$, with $f \in (0,1,2)$ corresponding to the cutoff regime, the saturation and the linear regimes respectively. $g_f(0,-e)$ is the normalized nonlinear function expressing the drain-source current in the three different regions of functioning of the $JFET$ at possible equilibrium points.

Nature of P0 at the cutoff region. The $JFET$ functions in the cutoff region for $x_1 \le x_m$, $\Rightarrow x_1^* = 0 \le x_m$, and $g_f(0,-e) = 0$. This is impossible since $x_m \prec 0$ as indicated after Eq. (4). Therefore, the point $P_0 = (0, e, 0, 0)$, cannot be defined as an equilibrium point.

Nature of P1 in the saturation region. The saturation regime of the transistor corresponds to $y_1 \le x_m$ and $e \ge -x_m$ et $g_1(0,-e) = x_m^2$. The related equilibrium point is $P_1 = \left(0, -e, 0, \frac{a_3}{a_1} x_m^2\right)$ and the corresponding Jacobian matrix is

$$M_{J_1} = \begin{bmatrix} -a_2 + 2a_3 x_m & 0 & -a_1 & a_1 \\ -2\alpha a_3 x_m & 0 & 0 & -\alpha a_1 \\ b_1 & 0 & 0 & 0 \\ -b_2 & b_2 & 0 & 0 \end{bmatrix} \quad (7)$$

Hence, the eigenvalues of the Jacobian matrix M_{J_1} are solutions of the following fourth order nonlinear algebraic equation in λ:

$$\lambda^4 + (a_2 - 2a_3 x_m)\lambda^3 + a_1(\alpha b_2 + b_2 + b_1)\lambda^2 + \alpha a_1 a_2 b_2 \lambda + \alpha a_1^2 b_1 b_2 = 0 \quad (8)$$

Considering the parameters,

$C_{GS} = 3.736\,pF, C_{GD} = 3.35\,pF, I_S = 33.57\,fA, V_{GSoff} = -1.409V, V_T = 25mV, g_{m0} = 1.754mAV^{-2}$, $I_0 = 1mA$, $w_0 = 10^9 rad/s, L_1 = 24.5\mu F, 104 \prec e \prec 149$, and $2.6V \prec E \prec 3.7V$, then solutions to Eq. 8 are : $\lambda_1 = -119.49, \lambda_2 = -15.87, \lambda_3 = 1.53 + 6.37i, \lambda_4 = 1.53 - 6.37i$.

Obtained results indicate that the treated equilibrium point is unstable, and P_1 can be called a spiral saddle index 2, in comparison to reference [25].

Nature of equilibrium point P_2 in the triode region If $y_1 \geq x_m$, hence $e \leq -x_m$. The $JFET$ functions in the linear regime and $g_2(0,-e) = -e(2x_m + e)$.

The second equilibrium point is $P_2 = \left(0, -e, 0, -\frac{a_3}{a_1} e(2x_m + e)\right)$. Its corresponding Jacobian matrix is

$$M_{J_2} = \begin{bmatrix} -a_2 + 2a_3 x_m & -2a_3(e + x_m) & -a_1 & a_1 \\ -2\alpha a_3 x_m & 2\alpha a_3(e + x_m) & 0 & -\alpha a_1 \\ b_1 & 0 & 0 & 0 \\ -b_2 & b_2 & 0 & 0 \end{bmatrix} \quad (9)$$

The eigenvalues of the Jacobian matrix M_{J_2} are solutions of the following fourth order nonlinear algebraic

$$\lambda^4 + (a_2 - 2\alpha a_3 e - 2a_3 x_m - 2\alpha a_3 x_m)\lambda^3 + (a_1 b_1 + a_1 b_2 + \alpha a_1 b_2 - 2\alpha a_2 a_3 x_m - 2\alpha a_2 a_3 e)\lambda^2 - \alpha a_1(2a_3 b_1 x_m + 2a_3 b_1 e - a_2 b_2)\lambda + \alpha a_1^2 b_1 b_2 = 0 \quad (10)$$

considering the same values of parameters, the solutions of $Eq.(10)$ are:

$$\lambda_1 = 1.21 + 37.95i, \lambda_2 = 1.21 - 37.95i, \lambda_3 = 5.47 + 5.16i, \lambda_4 = 5.47 - 5.16i.$$

As all the roots are complex conjugate with positive real parts, it reveals that P_2 is an unstable focus called a spiral repellor [25].

The unstable nature of the equilibrium points P_1 and P_2 supports the fact that the oscillator can oscillate chaotically.

2.2. Chaotic dynamic of Colpitts oscillator

The Colpitts oscillator (Figure 3) which has a typical common-base configuration is described by a set of three autonomous state-space equations [12]:

$$\begin{cases} \dot{x}_2 = y_2 - aF(z_2) \\ \dot{y}_2 = c - x_2 - z_2 - by_2 \\ \dot{z}_2 = y_2 - d \end{cases} \quad (11)$$

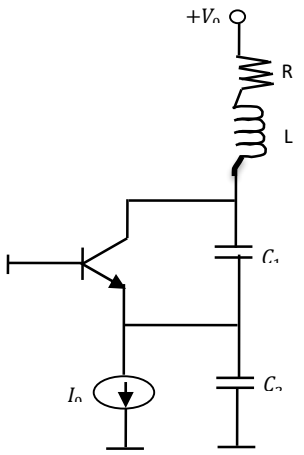

Figure 3: The circuit diagram of standard chaotic Colpitts oscillator

The variables and parameters of the system are defined as:

$$x = \frac{V_{C_1}}{V^*}, y = \frac{\rho I_L}{V^*}, z = \frac{V_{C_2}}{V^*}, t' \to t/\tau$$

$$\rho = \sqrt{\frac{L}{C_1}}, \tau = \sqrt{LC_1}, \varepsilon = \frac{C_2}{C_1}, a = \frac{\rho}{r}, b = \frac{R}{\rho}, c = \frac{V_0}{V^*}, d = \frac{\rho I_0}{V^*}$$

The normalized time is defined as in the previous Section 2.1.

Here r is the differential resistance of the forward-biased base–emitter junction and V^* is the break-point voltage of its I–V characteristics (for silicon transistors $V^* \approx 0.7$). In Equation 13, the collector current is assumed to be equal to the emitter current, i.e., the base current is neglected. The parameter c does not influence dynamical behavior of the oscillator, it sets only the components of the variables. Therefore, it can be omitted for simplicity. Two linear segments are used to approximate the I–V characteristic of the base–emitter junction:

$$F(z_2) = \begin{cases} -(1+z_2) & if \quad z_2 \succ -1 \\ 0 & if \quad z_2 \le -1 \end{cases} \tag{12}$$

Under the following parameters, $a = 15.5, b = 0.67, d = 0.96$ and $\varepsilon = 1$, the standard Colpitts oscillator exhibits chaotic oscillations as shown in Figure 4, with the initial conditions $(x(0), y(0), z(0)) = (0.2, 0.5, 0.5)$.

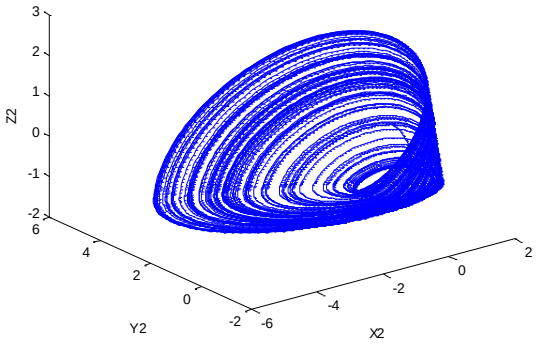

Figure 4: The simulated phase portrait in the space $[x_2, y_2, z_2]$ for $a = 15.5, b = 0.67, d = 0.96$

3. Chaos synchronization between Hartley and Colpitts oscillators with different orders

The objective in this section is to build a controller to ensure synchronization between Hartley and Colpitts oscillators operating in microwave frequencies range. In the literature, several methods to investigate the stability of the synchronization dynamics are proposed in the literature. Our approach is based on the adaptive observer method to adaptively synchronize between the nonlinear oscillators given by 4 and 10. Therefore, we define the dynamics of the synchronization error, and then, develop a control law that ensures the stability of all states and signals in the closed-loop system.

In order to observe the synchronization behavior in the two different Colpitts oscillators, we assume that the Hartley oscillator is the drive system and the Colpitts oscillator is the response system, indicated by subscription 1 and 2 as

$$\begin{cases} \dot{x}_1 = a_1(v_1 - z_1) - a_2\left[\exp(x_1) - 1\right] - a_3 g(x_1, y_1) \\ \dot{y}_1 = \alpha\left(a_1 v_1 - a_3 g(x_1, y_1)\right) \\ \dot{z}_1 = b_1 x_1 \\ \dot{v}_1 = b_2(e - x_1 + y_1) \end{cases} \tag{13}$$

and

$$\begin{cases} \dot{x}_2 = y_2 - aF(z_2) + u(t) \\ \dot{y}_2 = c - x_2 - z_2 - by_2 \\ \dot{z}_2 = y_2 - d \end{cases} \tag{14}$$

respectively, where $u(t)$ represents the control action to be designed.

Let us define the dynamics of the synchronization error as follows

$$e_1 = z_2 - z_1$$

$$e_2 = y_2 - k_1$$

$$e_3 = x_2 - k_2$$

where k_1 and k_2 are some given variables in function of the two systems variables.

Remark 1. One notes that we use only one controller; this will allow considerably reduced parameters estimation and synchronization achievement time.

Our goal is therefore to determine the control function $u(t)$ to ensure chaos synchronization between the two systems. The only requirement imposed here is that the two variables k_1 and k_2 have to be bounded by upper bounds, which are not needed to be known. The knowledge of these upper bounds will be overcome by the adaptive laws proposed in the following theorem.

Theorem 1. Consider the master and slave oscillators represented by (13) and (14). If the control action is designed as follows

$$u(t) = -\eta e_3 + e_2 - w(t) \tag{15}$$

in which the adaptation laws are designed by

$$k_1 = -\lambda e_1 + b_1 x_1 + d \tag{16}$$

$$k_2 = e_1 + \eta e_2 + (\lambda - b) y_2 - z_2 - b_1 \lambda x_1 + a_2 b_1 \left[\exp(x_1) - 1\right] - a_1 b_1 (v_1 - z_1) - a_3 b_1 g(x_1, y_1) - \lambda d \tag{17}$$

$$w(t) = y_2 - aF(z_2) - \dot{k}_2 \tag{18}$$

Then the stability of the closed-loop system can be guaranteed. Moreover, convergence of the synchronization errors can be made arbitrarily small by adjusting the parameters gains μ, λ and η.

Proof 1. We construct a Lyapunov function candidate according to the different variables. Accordingly, from systems (13) and (14), we obtain: $\dot{e}_1 = y_2 - b_1 x_1 - d$.

Constructing the first partial Lyapunov function as: $V_1 = \frac{1}{2} e_1^2$, the derivative part of derivation of this function is obtained as follows :

$$\dot{V}_1 = e_1\dot{e}_1 = -\lambda e_1^2 + e_1\left(y_2 + \lambda e_1 - b_1 x_1 - d\right) \tag{19}$$

when $\lambda \succ 0$ is a constant value introduced in order to construct a first negative part of derivative of Lyapunov function.

On other hand, we have $\dot{e}_2 = \dot{y}_2 - \dot{k}_1$. Using formulas (13) and (14) we get

$$\dot{e}_2 = -x_2 + (\lambda - b)\, y_2 - z_2 - b_1\lambda x_1 + a_2\left[\exp(x_1) - 1\right] - a_1 b_1\left(v_1 - z_1\right) - a_3 g\left(x_1, y_1\right) - \lambda d$$

The second partial Lyapunov function is constructed as follows

$$V_2 = V_1 + \frac{1}{2}e_2^2$$

One gets:

$$\dot{V}_2 = \dot{V}_1 + e_3\dot{e}_3 = -\lambda e_1^2 - \eta e_2^2 + e_2\left(-x_2 + e_1 + \eta e_2 + (\lambda - b) y_2 - z_2 - b_1\lambda x_1 + a_2 b_1\left[\exp(x_1) - 1\right] - a_1 b_1\left(v_1 - z_1\right) - a_3 b_1 g\left(x_1, y_1\right) - \lambda d\right) \tag{20}$$

where $\eta \succ 0$

Finally, the dynamics error $\dot{e}_3$ is derived from (13) and (17) as follows

$$\dot{e}_3 = \dot{x}_2 - \dot{k}_2 = y_2 - aF\left(z_2\right) + u(t) - \dot{k}_2 = u(t) + w(t)$$

$$\dot{e}_3 = y_2 - aF\left(z_2\right) - \dot{e}_1 - \eta\dot{e}_2 - (\lambda - b)\,\dot{y}_2 + \dot{z}_2 + b_1\lambda x_1 - a_2\dot{x}_1\left[\exp(x_1) - 1\right] - a_1 b_1\left(\dot{v}_1 - \dot{z}_1\right) + a_3 g\left(x_1, y_1\right) \tag{21}$$

Where

$$g'\left(x_1, y_1\right) = \begin{cases} 0 & if \quad x_1 \le x_m \\ 2\dot{x}_1\left(x_1 - x_m\right) & if \quad y_1 \le x_m \\ \left(\dot{x}_1 - \dot{y}_1\right)\left(x_1 + y_1 - 2x_m\right) + \left(x_1 - y_1\right)\left(\dot{x}_1 + \dot{y}_1\right) & if \quad y_1 \ge x_m \end{cases} \tag{22}$$

The last Lyapunov function is then constructed as

$$V = V_2 + \frac{1}{2}e_3^2$$

Then, the derivative of V is:

$$\dot{V}_3 = \dot{V}_2 + e_3\dot{e}_3 = -\lambda e_1^2 - \eta e_2^2 - \mu e_3^2 + e_3\left(\mu e_3 - e_2 + u(t) + w(t)\right) \tag{23}$$

$$\dot{V}_3 = -\lambda e_1^2 - \eta e_2^2 - \mu e_3^2 + e_3\left(\mu e_3 - e_2 + w(t) - \mu e_3 + e_2 - w(t)\right)$$

where $\mu \succ 0$. Substituting $Eq.(15)$, we get :

$$\dot{V}_3 = -\lambda e_1^2 - \eta e_2^2 - \mu e_3^2 \prec 0 .$$

Hence, the time derivative $\dot{V}_3$ is negative as long as the term in braces is positive. According to Lyapunov stability theory, the synchronization of the two systems is then achieved and the error variables of the system $e_i(t)$approach zero with the lapses of times, i.e.,

$$\lim_{t\to 0} e_i\left(t\right) = 0 \qquad \left(i = 1,2,3\right)$$

This completes the proof.

Corollary 1. The following variables

$$\begin{cases} H_1\left(x_1, y_1, z_1\right) = z_1 \\ H_2\left(x_1, y_1, z_1\right) = b_1 x_1 + \lambda z_1 + d \\ H_3\left(x_1, y_1, z_1\right) = -2b_1\lambda x_1 + a_2 b_1 \exp(x_1) - a_1 b_1\left(v_1 - z_1\right) - a_3 b_1 g\left(x_1, y_1\right) - \left(\lambda + \eta\right)d - a_2 \end{cases} \tag{24}$$

And

$$\begin{cases} S_1\left(x_2, y_2, z_2\right) = z_2 \\ S_2\left(x_2, y_2, z_2\right) = y_2 + \lambda z_2 \\ S_3\left(x_2, y_2, z_2\right) = x_2 - \left(\lambda + \eta - b\right)y_2 - \lambda\eta z_2 \end{cases} \tag{25}$$

Are considered as observable variables of systems (13) and (14) only if the errors

$$\begin{cases} e_1 = z_2 - z_1 = S_1\left(x_2, y_2, z_2\right) - H_1\left(x_1, y_1, z_1\right) \\ e_2 = y_2 - k_1 = S_2\left(x_2, y_2, z_2\right) - H_2\left(x_1, y_1, z_1\right) \\ e_3 = x_2 - k_2 = S_3\left(x_2, y_2, z_2\right) - H_3\left(x_1, y_1, z_1\right) \end{cases}$$

Verify that

$$\lim_{t\to 0} e_i(t) = \lim_{t\to\infty}\left(S_i(x_2, y_2, z_2) - H_i(x_1, y_1, z_1)\right) = 0,\ (i = 1,2,3)$$

The construction of observable variables completes the method.

4. Computer experiments

We have theoretically showed that the systems (13) and (14) which respectively represent Hartley and Colpitts oscillators can be synchronized if the controller is of the form (15). This controller has been derived by constructing progressively the error equations and the Lyapunov functions. To verify the effectiveness of the proposed control technique, let the drive system with initial conditions $(0.02,-8.16,-0.84,0.42)$ and the response system with initial conditions $(0.2, 0.5, 0.5)$. The parameters $a_1 = 10.706638, a_2 = 0.000036$, $a_3 = 0.011737$,

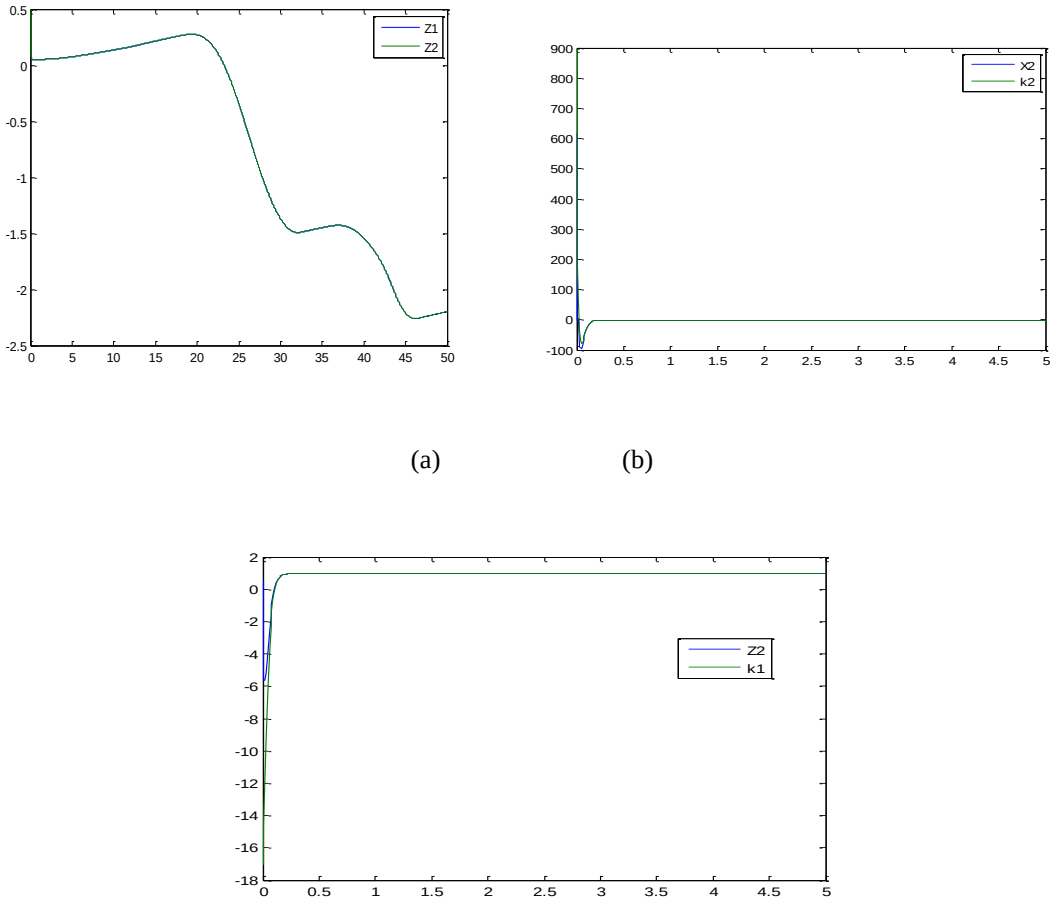

(a) (b)

(c)

Figure 5: Evolution of the state variables of the master and slave systems in the presence of the controller

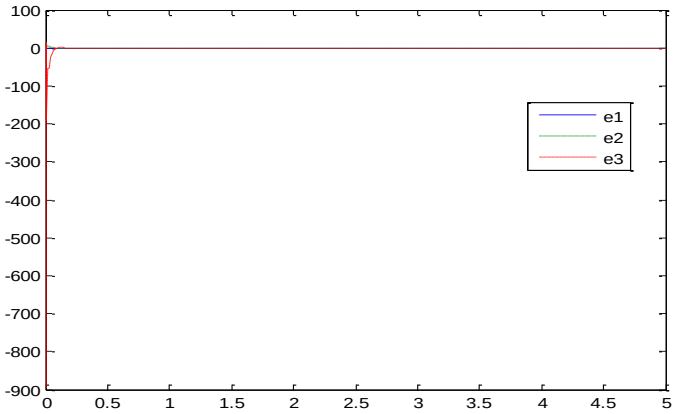

Figure 6: Graphs of synchronization errors e_1, e_2, e_3 with normalized time t ($\lambda = \eta = \mu = 20$)

$b_1 = 0.001020, b_2 = 0.00625$, $b = 0.67, d = 0.96, \alpha = 1.115223, \varepsilon = 1, x_m = -56.36$, are keep constants during present computations.

Choosing appropriated values for λ, η, μ is very important. For $\lambda = \eta = \mu = 20$, Figures. 5 and 6 display the good results for synchronization. Computer experiments show that synchronization is achieved successfully and the error signals approach zero smoothly and quickly. We have solved numerically Equations (13) and (14) using the fourth-order Runge–Kutta algorithm with a time step $\Delta t = 0.01$.

5. Discussion of results

The numerical results clearly demonstrate the effectiveness of the proposed adaptive observer–based method for synchronizing two non-identical chaotic oscillators of different orders operating in the UHF band. In particular, successful synchronization between the fourth-order Hartley oscillator and the third-order Colpitts oscillator is achieved using a single control input, which represents a significant advantage over many existing approaches that require multiple control laws or full knowledge of system parameters.

Numerical simulations show that the synchronization errors converge rapidly to an arbitrarily small neighborhood of zero, thereby confirming the robustness of the proposed control strategy. This convergence is achieved despite the structural dissimilarity of the oscillators, the presence of strong inherent nonlinearities associated with electronic components, and the absence of any prior knowledge of the upper bounds of the internal system signals.

The use of Lyapunov stability theory provides a rigorous proof of closed-loop system stability. The introduced adaptive laws effectively compensate for dynamic uncertainties and enable online estimation of unknown terms, making the proposed approach particularly well suited for real electronic systems operating at high frequencies. Moreover, synchronization is achieved without requiring an exhaustive parameter identification process, which further enhances the practical relevance of the method.

Another important outcome of this study is that synchronization is successfully realized in the UHF band, a frequency range in which the generation and control of chaotic signals remain particularly challenging. This feature significantly increases the potential applicability of the proposed scheme, especially in secure communication systems, chaotic radar applications, and advanced microwave technologies.

Finally, the choice of Hartley and Colpitts oscillators is motivated by practical considerations. These architectures are widely used and technologically accessible, making them realistic platforms for future experimental implementation of the proposed synchronization scheme and thereby strengthening the practical impact of the reported results.

6. Constraints and Limitations of the Study

Despite the encouraging results, several limitations of this study should be acknowledged.

First, the findings are based exclusively on numerical simulations using normalized mathematical models. No experimental validation has been carried out at this stage, and certain phenomena inherent to real electronic circuits such as thermal noise, component tolerances, temperature drift, and parasitic electromagnetic couplings have not been taken into account.

Second, the modeling of the active electronic components relies on piecewise-linear nonlinear approximations. While these models are commonly adopted for dynamical analysis and control design, they may deviate from the actual behavior of electronic devices, particularly at very high operating frequencies.

Furthermore, the influence of explicit external disturbances, such as measurement noise or radio-frequency interference, has not been considered. Therefore, a comprehensive robustness analysis of the proposed synchronization scheme in the presence of such perturbations remains an open research direction.

Finally, although the synchronization errors can be made arbitrarily small through appropriate tuning of the adaptive gains, no systematic optimization procedure for selecting these parameters is provided. In addition, the achieved synchronization is of a practical nature, characterized by convergence to a bounded neighborhood of the synchronized state rather than strict asymptotic convergence. Nevertheless, this level of synchronization is generally sufficient for most physical and technological applications.

7. Conclusion

In this work, we have investigated the synchronization of non-identical chaotic oscillators of different orders operating in the UHF band using an adaptive observer-based approach.

Synchronization between a fourth-order Hartley oscillator and a third-order Colpitts oscillator was successfully achieved despite strong nonlinearities and structural differences.

A Lyapunov-based adaptive control law was designed to ensure closed-loop stability and convergence of the synchronization errors using a single control input, without requiring prior knowledge of system parameters. Numerical simulations confirm the effectiveness and robustness of the proposed method, demonstrating reliable chaos synchronization at ultra-high frequencies.

These results highlight the potential of adaptive observer techniques for high-frequency chaotic systems and provide a promising framework for applications in secure communications and microwave technologies.

References

[1] L. M. Pecora and T. L. Carroll. "Synchronization in chaotic systems". *Phys. Rev. Lett.* Vol. 64, pp. 821-824, 1990.

[2] Terry J.R and Vanwiggeren G.D. "Chaotic communication using generalized synchronization". *Chaos Solitons Fractals*. Vol. 12, pp. 145-152, 2001.

[3] Guo X. W and Shu L. Q. "Chemical chaotic schemes derived from NSG system". *Chaos Solitons Fractals*. Vol. 15, pp. 663-671, 2003.

[4] Petrovskii S., Li. B. L. and Malchow H. "Quantification of spatial aspect of chaotic dynamic in biological and chemical systems*". Bull. Math. Boil*. Vol. 65, pp. 425-446, 2003.

[5] Kennedy MP. "Chaos in the Colpitts oscillator". *IEEE Trans Circ Syst I*, Vol. 41, pp.771–784.

[6] Wegener C, Kennedy MP. "RF chaotic Colpitts oscillator". In Proc. of an international workshop on nonlinear dynamics of electronic systems NDES, Dublin Ireland, 1995, pp. 255–8.

[7] Mykolaitis G, Tamasevicius A, Bumeliene S. "Experimental demonstration of chaos from the Colpitts oscillator in the VHF and the UHF ranges". *Electron Lett*, Vol. 40, pp. 91–2, 2004.

[8] Elwakil AS, Kennedy MP. "Construction of classes of circuit- independent chaotic oscillators using passive-only nonlinear devices". *IEEE Trans*. Vol. 48, pp. 289-307, 2001.

[9] Elshabini-Riad Aicha, Stephenson F. W, Bhutta Imran. "*Electrical Equivalent Circuit Models and Device Simulators for Semiconductor Devices*". In Dorf Richard C., editor. The Electrical Engineering Handbook. Boca Raton: CRC Press LLC, 2000.

[10] Tamasevicius A, Cenys A, Mykolaitis G, Namajunas A. "Synchronization of chaos and its application to secure communication". *Lithuanian J Phys*, Vol.38, pp.33–7, 1998.

[11] Uchida A, Kawano M, Yoshomori S. "Dual Synchronization of chaos in Colpitts electronic oscillators and its applications for communications". *Phy. Rev.* Vol. 68:56207:1–056207:11.

[12] Qiao S, Shi ZG, Chen KS, Cui WZ, Ma W, Jiang T, et al. "A new architecture of UWB radar utilizing microwave chaotic signals and chaos synchronization". *Prog Electromagnetics Res PIER*, 2007, Vol. 75, pp. 225–37.

[13] Tamasevicius A, Mykolaitis G, Bumeliene S, Cenys A, Lindberg E.. "*Synchronization of VHF chaotic Colpitts oscillator, in: Proceedings 17of international workshop on nonlinear dynamics of electronic systems NDES'97"*. Delft Netherlands; pp. 223–6, 2001.

[14] Rubezic V, Ostojic R. "*Synchonization of chaotic Colpitts oscillator with applications to binary communications*". In Proc. *ICECS*, 1999, pp. 153–6.

[15] Burykin VA, Panas AI (1997). "Chaotic synchronization of RF generators". *In Proc. NDES* 1997, Moscow Russia; pp. 548–53.

[16] Baziliauskas A, Krivickas R, Tamasevicius A. "*Coupled chaotic Colpitts oscillator: identical and mismatched cases*". Nonlinear Dynam, Vol. 44, pp. 151–8, 2006.

[17] Fotsin HB, Daafouz J. "*Adaptive synchronization of uncertain chaotic Colpitts oscillators based on parameter identification*". Phys Lett A, Vol. 339, pp. 304–15, 2005.

[18] Li GH. "*Synchronization and anti-synchronization of Colpitts oscillators using active control*". Chaos Soliton Fract, Vol. 26, pp. 87–93, 2005.

[19] Cenys A, Tamasevicius A, Mykolaitis G. "Hyperchaos and synchronization in mean field coupled chaotic oscillator". In Proc. *NOLTA*, 1998, Crans-Montana Switzerland; pp. 519–40.

[20] Li GH. "*Chaos and synchronization of Colpitts oscillators*". Microwave Opt Technol Lett, Vol. 39, pp. 446–9, 2003.

[21] Liao TL, Tsai SH. "*Adaptive synchronization of chaotic systems and its application to secure communications*". Chaos Soliton Fract, Vol. 11, pp. 1387–96, 2000.

[22] L¨u L, Luan L, Guo ZA (2007). "*Synchronization of chaotic systems with different orders*". Chin Phys, Vol. 16, pp. 06–346.

[23] Baars G. "*Hartley-oscillatormitnurzweiBauteilen*".Elektor.Vol.29, pp.7-8. 18, 2002.

[24] Attia J. O. "Transistor circuits". *In Attia John Okyere, editor.Electronics and circuits analysis using MATLAB,* 1999. Boca Raton: CRC Press LLC.

[25] Sprott J. C. "Chaos and time-series analysis". *New York: Oxford University Press*, 2003.

[26] Chua L. O. (1992). "*The genesis of Chua's circuit*". Stuttgart: HirzelVerlag. AEU 46, pp. 250-257.